Measures for Reliable and Effective Operation of a Conical Fluidized-Bed Combustor Fired with Oil Palm Shells: A Cold-State Hydrodynamic Study

Pichet Ninduangdee and Vladimir I. Kuprianov*

School of Manufacturing Systems and Mechanical Engineering, Sirindhorn International Institute of Technology, Thammasat University, Pathum Thani 12121, Thailand
*Corresponding Author: E-mail address: ivlaanov@siit.tu.ac.th; tel.: +66 2 986 9009, ext. 2208; fax: +66 2 986 9112

Abstract

This work is the first part of a comprehensive experimental study on burning of shredded oil palm shells in a conical fluidized-bed combustor (FBC) using alumina sand as the bed material. Hydrodynamic regimes and characteristics of pure alumina as well as of a binary (alumina–biomass) mixture fluidized by ambient air were studied on a conical part of the combustor using two size groups of biomass particles. For each size group, the test runs were performed for different static bed heights at variable biomass fraction in the mixture. Air was injected into the bed through the modified bubble-cap air distributor ensuring a rather low pressure drop across the distributor and uniform airflow over the bed. In a particular trial, the pressure drop across the bed (Δp) was measured versus superficial air velocity at the distributor exit (u). The Δp-u diagrams were plotted for the ranges of operating variables with the aim to determine major hydrodynamic characteristics of the bed: the minimum velocity of partial fluidization (u_{mpf}) and the minimum velocity of full fluidization (u_{mff}). In all trials, four sequent hydrodynamic regimes of the bed were found to occur when increasing u from of 0 to 6 m/s. Both u_{mpf} and u_{mff} as well as corresponding pressure drops (Δp_{max} and Δp_{mff}) were found to be in quasi-liner correlations with static bed height, whereas the particle size and the percentage of shredded shells in the binary mixture showed only minor effects on these characteristics. The dimensionless dependencies of $\Delta p/\Delta p_{max}$ on u/u_{mpf} for all the trials were found to exhibit strong similarities. A static bed height of 30 cm can be recommended for the conical FBC as ensuring stable fluidization of the bed as well as sustainable fuel ignition.
***Keywords**:* Conical fluidized bed; Alumina–biomass mixture; Hydrodynamic regimes and characteristics.

1. Introduction

Hydrodynamic characteristics of a gas–solid bed are key input parameters for optimal design and operation of a fluidized-bed combustion system (furnace/combustor), as well as for proper selection of system auxiliary equipment [1].

A large number of research studies have been addressed hydrodynamic regimes and characteristics of columnar (cylindrical/prismatic) bubbling fluidized gas–solid beds [2,3] widely used in fluidized-bed combustion systems. The minimum fluidization velocity, u_{mf}, and the corresponding pressure drop across the bed, Δp_{mf}, are reported to be major hydrodynamic characteristics of these conventional (columnar) fluidized-bed systems. As revealed by cold-state experimental studies using various bed materials, u_{mf} is a function of the bed density, particle size, sphericity and voidage, showing no effects of static bed height, while Δp_{mf} is in a quasi-liner correlation with bed weight (height) and inversely proportional to cross-sectional area of the bed.

Hydrodynamics of tapered (or wedge-like) and conical fluidized beds is reported to be more complicated and therefore characterized by a greater number of hydrodynamic regimes and characteristics compared to those of columnar fluidized beds. Because of a negative velocity gradient along the bed height, the fluidization characteristics of a conical gas–solid bed are sensibly affected by the static bed height, and this influence is strongly dependent on the bed particle size [1,4,5]. Due some apparent advantages, such as a lesser amount of the bed material and lower pressure drop across the fluidized bed (Δp) than those of cylindrical and prismatic beds of similar height, a fluidized-bed combustion system with a cone-shape bed seems to be a promising technique for effective and reliable burning of various biomass fuels at minimal operational costs [6,7].

However, with its irregular shape and size of individual particles, biomass has a significant impact on the bed behavior in a real combustion system injecting the fuel into/over the fluidized bed. The hydrodynamic characteristics of binary mixtures fluidized in columnar beds have been reported by some research studies [8,9]. As revealed in these studies, the hydrodynamic behavior of a fluidized bed with the binary mixture is sensibly influenced by properties of both biomass and bed material, the major effects being produced by the density and particle size of the two solids.

Effects of the weight percentage of biomass on the hydrodynamic characteristics of a binary (alumina–cotton stalk) mixture fluidized in the bed of variable cross-sectional area was investigated by Sun et al. [10]. It was found that u_{mf} had a trend to be increased as the percentage of biomass in the bed was increased, likely due to an increase in the bed voidage. In the meantime, Δp_{mf} apparently decreased when increasing the proportion of biomass in the mixture, mainly due to the reduced bed weight.

Oil palm residues are largely produced by the Thai palm oil industry and represent, in effect, important and promising biomass resources in Thailand. However, all oil palm residues, including oil palm shells, exhibit high risks of (i) bed agglomeration and accumulation (leading eventually to the bed defluidization), and also (ii) ash deposition on reactor walls when burning these high-alkali biomasses a fluidized bed and using a typical bed material (silica sand). In order to avoid these ash-related problems, alternative bed materials, such as alumina sand or other alumina-rich materials, can be used in fluidized-bed combustion systems [7,10,11]. A conical fluidized-bed combustor (FBC) ensuring the bed fluidization at a minimal amount of the bed material seems to be an appropriate combustion technique for testing and using costly alternative bed materials [7].

The main objective of this cold-state study was to examine the behavior of alumina sand, as well as of mixtures of alumina sand and oil palm shells, in a conical bed for variable superficial air velocity at the air distributor exit (u). Effects of static bed height and biomass fraction in the binary mixture on the major hydrodynamic regimes and characteristics, as well as on the entire Δp-u diagram of the conical air–solid bed, were the main focus of this experimental study.

2. Materials and Methods

2.1 Experimental set up

Cold-state hydrodynamic tests were performed on a special experimental model (reproducing a bottom part of the conical FBC) depicted in Fig 1. The experimental rig consisted of two sections: (1) a conical section with a 40° cone angle and 0.25 m inner diameter at the bottom base, and (2) a cylindrical section of 2 m height and 1 m inner diameter. An air blower was used to supply ambient air (fluidizing agent) to the rig through an air pipe of 0.1 m inner diameter.

Air was injected into the bed (with alumina sand or alumina–biomass mixture) through the modified air distributor shown in Fig. 2. The distributor consisted of nineteen bubble caps

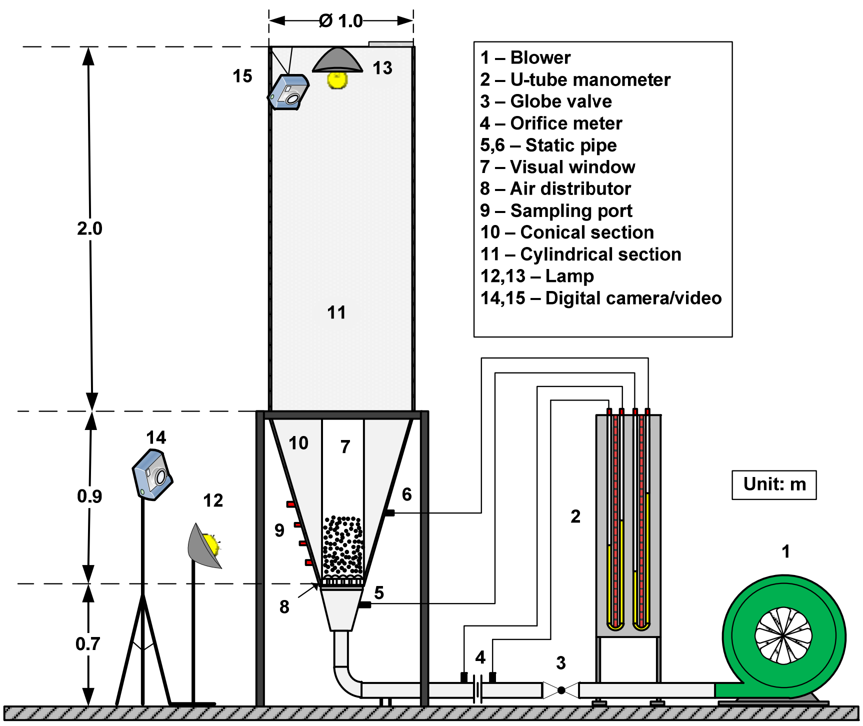

Fig. 1 Schematic diagram of the experimental set up for the cold-state hydrodynamic study

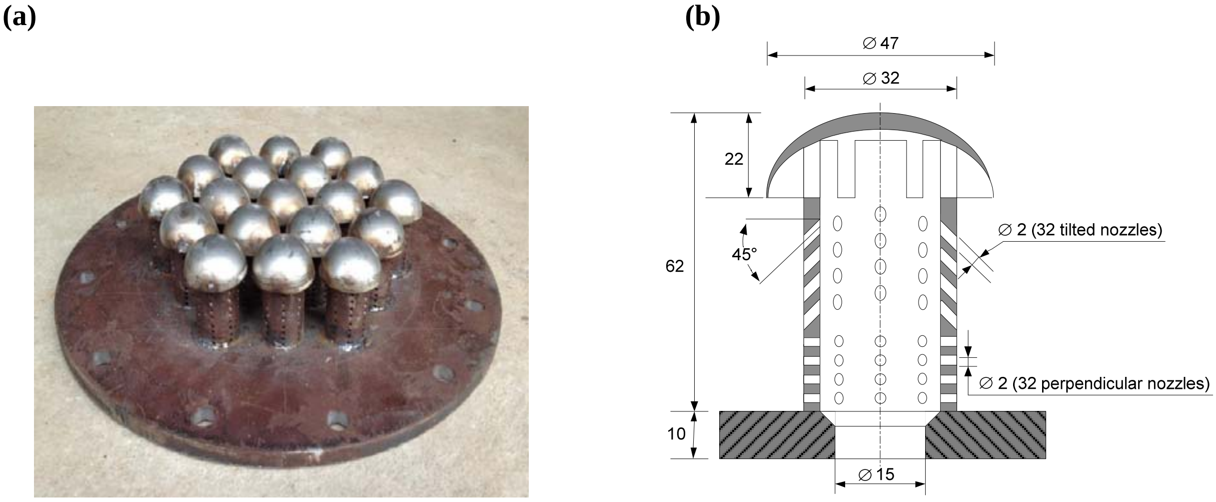

Fig. 2 (a) A bubble-cap air distributor and (b) geometrical details of an individual bubble cap

arranged on the air distributor plate, as shown in Fig. 2a. Such an air distributor design ensures a rather uniform distribution of airflow between the bubble caps and, thus, over the air distributor.

An individual stand pipe depicted in Fig. 2b had sixty four holes each of 2 mm in diameter, distributed evenly over the pipe surface, and also six vertical slots with 3 mm width and 15 mm height located under the cap of 47 mm diameter (see Fig. 2b). The net cross-sectional area of airflow at the distributor exit (calculated as the difference between the area of the 0.25-m-diameter distributor plate and the total area occupied by the caps) was $A_{\mathrm{air}} = 0.016\ \mathrm{m}^2$.

The rate of airflow (Q_{air}) was adjusted by a globe valve downstream from the blower, and this operating variable was controlled by using an orifice-type flowmeter equipped with a U-tube manometer (see Fig. 1). A multifunction flowmeter “Testo-512” with the L-type Pitot tube was used to measure air velocity across the air pipe in the calibration tests. A relationship between the airflow rate (Q_{air}) (quantified in these set-up tests by integrating the velocity profile across the air pipe) and the valve opening, was determined prior to the experimental study. For the particular operating conditions (i.e., for the particular test run), the superficial air velocity at the distributor exit was then quantified as $u = Q_{\mathrm{air}}/A_{\mathrm{air}}$

The total pressure drop across the distributor–bed system (Δp), comprising the air–solid bed and the air distributor (AD), was measured for variable superficial air velocity (u) by using another U-tube manometer with two static pressure tubes: one tube was arranged in the air duct below the air distributor, while the second one was fixed over the bed, as shown in Fig. 1.

2.2 Experimental procedure

Alumina sand with the solid density of about 3500 kg/m^3 and (sieved) particle sizes of 0.3–0.5 mm was used as the bed material sustaining bed fluidization. Prior to tests with mixtures, oil palm shells (OPS) were shredded to ensure stable fuel feeding when burning shell-type biomass fuels in the conical FBC, as recommended in Ref. [7].

Hydrodynamic regimes and characteristics of pure alumina sand as well as of a binary (alumina–biomass) mixture were determined in this study via analysis of Δp-u diagrams plotted for various operating conditions. Note that the tests with pure alumina were performed for both fluidization (via increasing u) and defluidization (via decreasing u) of the bed, whereas trails with binary mixtures were limited by the runs for bed fluidization, because of segregation of alumina and biomass particles during the bed fluidization.

To investigate the effects of biomass particle size, the trials with the binary mixtures were performed for two size groups of OPS particles: 3–6 mm and 7–10 mm. For trials of each size group, alumina sand was mixed with the shells in different mass fractions (MF) in the binary mixture: 0% (i.e., when using pure alumina), 2.5%, 5%, 7.5% and 10% (all by weight). Prior to the tests, alumina or binary alumina-OPS mixture was placed in the conical module forming a loosely packed bed. For given MF, the test runs were performed for three static bed heights (BHs): 20, 30 and 40 cm. When testing the bed with pure alumina, these BHs were ensured by alumina masses of 40, 65 and 98 kg, respectively. All the tests were performed at ambient temperature and atmospheric pressure at the air blower inlet.

For selected parameters (BH, MF and particle size of OPS), the pressure drop across the bed was measured versus superficial air velocity with the aim to provide data for plotting the Δp-u diagram of the conical bed, which, afterwards, was used for determining major hydrodynamic regimes and characteristics of the bed. In each test run, the superficial air velocity was ranged from 0 to up to 6 m/s to observe different hydrodynamic regimes of the bed, which may potentially occur in the conical FBC.

3. Results and Discussion

3.1 Hydrodynamic regimes and characteristics of alumina sand beds fluidized by ambient air

Fig. 3 shows the Δp-u diagram of the conical alumina bed of 30 cm static bed height for two experimental procedures: fluidization (solid symbols) and defluidization (open symbols).

It can be seen in Fig. 3 that with increasing the superficial air velocity, the pressure drop across the bed and air distributor varied following the path O→A→B→C. When increasing u, four sequent hydrodynamic regimes of bed behavior were basically observed during the test run for bed fluidization: (I) fixed-bed regime, (II) partially fluidized-bed regime, (III) fully fluidized-bed regime and (IV) turbulent fluidized-bed regime, as indicated in Fig. 3. These hydrodynamic regimes had much common with those found for the conical/tapered beds using various bed materials and fluidizing fluids [1,4,5].

With increasing u within the fixed-bed regime (O→A), Δp was found to be increased until the maximum value, Δp_{max}, was attained. At critical point A ($\Delta p = \Delta p_{max}$), the lowest layer of the conical alumina bed began to fluidize, as established by visual observations. Superficial air velocity giving the start to the partially fluidized-bed regime was therefore termed the minimum velocity of partial fluidization (u_{mpf}) [4]. During this regime (A→B), Δp abruptly reduced from Δp_{max} to Δp_b (the latter being substantially lower than Δp_{max}), whereas u exhibited a stepwise change from u_{mpf} to the value termed the minimum velocity of full fluidization (u_{mff}). At $u = u_{mff}$ (at point B), the entire bed was involved in fluidization exhibiting random appearance of small-size bubbles on the bed surface. Within the fully fluidization regime (B→C), with increasing u greater than u_{mff}, Δp stayed (almost) constant, due to quite low pressure drop across the air distributor even at highest u. It was observed that with higher superficial air velocity, the frequency of appearance and size of the bubbles released from the fluidized bed showed the trend to be increased. At the superficial air velocity at point C termed the minimum velocity of turbulent fluidization ($u = u_k$), the bed behavior turned abruptly into the turbulent fluidization regime, which was then observed at $u > u_k$ (within the specified range of air supply). During this regime, no bubbles were observed in the bed, which however exhibited a significant expansion (occupying the entire volume of the conical section) and turbulent gas–solid flow.

On the contrary, when superficial air velocity was decreased causing a gradual change in the bed behavior from the turbulent fluidization regime at point C* to its entire defluidization at point A* (where the superficial air velocity was reduced to the value termed the maximum velocity of full defluidization, u_{mfd}), the bed unavoidably passed point B* (where the upper

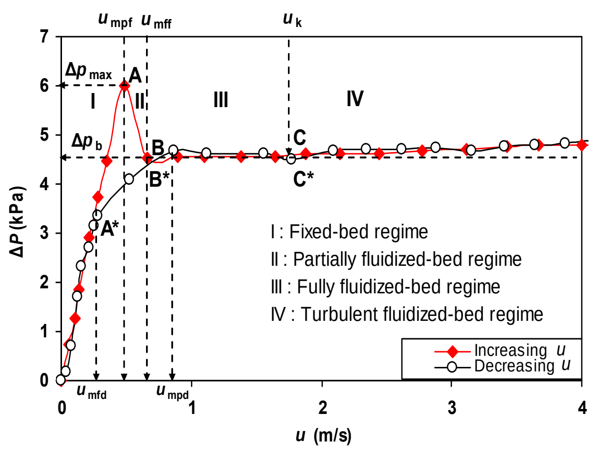

Fig. 3 Hydrodynamic regimes and characteristics of the conical alumina bed at BH = 30 cm for fluidization-defluidization procedures

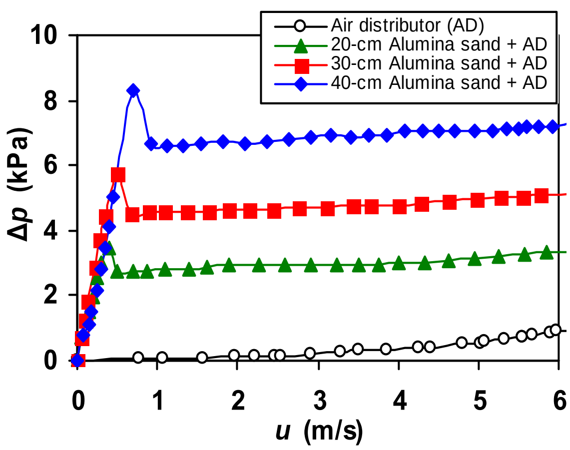

Fig. 4 Dependence of Δp on u for the air distributor (AD) and the Δp-u diagram of alumina beds for different BHs (including effects of AD)

layer of the bed was defluidized at the maximum velocity of partial defluidization, u_{mpd}) exhibiting the defluidization path C*→B*→A*→O in Fig. 3. Thus, during the fluidization-defluidization procedures, the conical bed with alumina sand of the selected properties showed an apparent hysteresis in the Δp-u diagram.

However, the Δp-u diagram of a defluidizing bed provides no useful information that could be used for combustor optimal design and operation, since at $u < u_{mpd}$, the bed doesn't exhibit full fluidization. For this reason and because of segregation of sand and biomass particles during turbulent and bubbling fluidization regimes, it was decided to use in this study the Δp-u diagrams (for variable bed properties and characteristics) from fluidization procedures only.

Fig. 4 shows the effects of BH on the Δp-u diagram of the conical bed when using pure alumina as the bed material (solid dots) and also the contribution of the pressure drop across the air distributor alone to the total Δp for variable u (open dots). As seen in Fig. 4, with increasing BH, the u_{mpf} and u_{mff}, and their corresponding pressure drops (Δp_{max} and Δp_b, respectively, as defined in Fig. 3) of the alumina bed showed the trend to be increased, mainly due to an increase in the bed weight. As can be observed in Fig. 4 that the contribution of this modified air distributor to the total Δp was relatively small, maximum ~0.9 kPa (at u = 6 m/s), compared to that of the previously used air distributor with thirteen bubble caps [7]. Such a result was mainly achieved due to the increased numbers of bubble caps as well as of vertical slots (i.e., increased total airflow area of all the bubble caps), which resulted in reduced friction losses and (eventually) pressure drop across the air distributor alone. In the meantime, from observation of bed behavior, the modified nineteen bubble-cap air distributor ensured the uniform distribution of airflow over the distributor plate and correspondingly across the fluidized bed, due to quite close arrangement of the bubble caps on the plate.

3.2 Hydrodynamics of alumina-biomass beds

Fig. 5 compares the Δp-u diagrams of conical beds of alumina mixed with shredded oil palm shells of 3–6 mm particle sizes at different static bed heights between the specified percentages of biomass in the binary mixture. It can be seen in Fig. 5 that all the Δp-u diagrams of the conical beds with binary mixtures exhibited similar

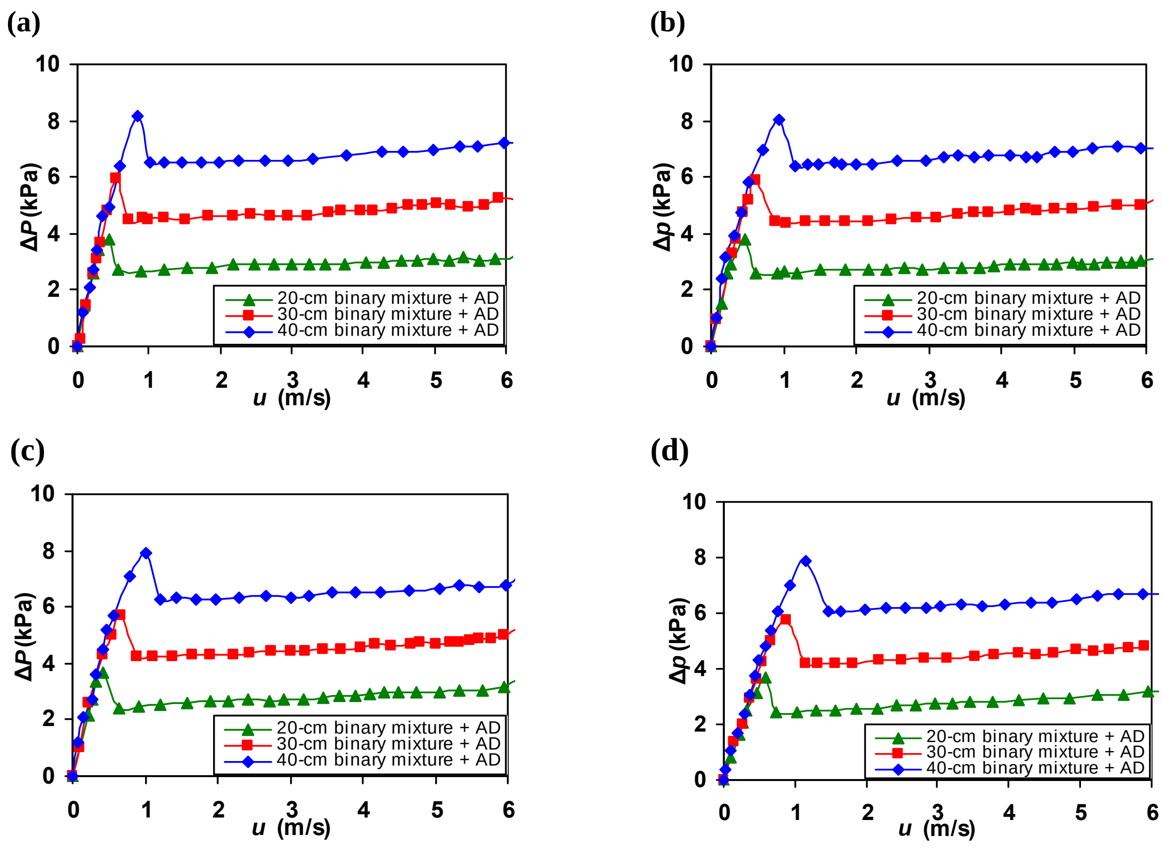

Fig. 5 Effects of static bed height on the Δp-u diagram of alumina mixed with shredded oil palm shells of 3−6 mm particle sizes for variable proportion of biomass in the binary mixture: (a) 2.5 wt.%, (b) 5.0 wt.%, (c) 7.5 wt.% and (d) 10 wt.%

hydrodynamic regimes and characteristics, as those determined for pure alumina conical beds during the fluidization procedures (see Fig. 3). However, with increasing the weight percentage of biomass in the binary mixture at a fixed BH, both u_{mpf} and u_{mff} showed a trend to be somewhat increased, and the effect from static bed height was strengthening with higher static beds. In the meantime, with greater proportion of biomass in the bed, the magnitudes of Δp_{max} and Δp_b showed a slight reduction at distinct (fixed) BHs. This fact can be explained by the reduction of total weight of the binary mixture when maintaining BH at a constant value. For instance, at BH = 30 cm, with increasing the percentage of biomass in the binary mixture from 2.5 wt.% to 10 wt.%, u_{mff} (an important characteristic of bed fluidization) increased from 0.8 m/s to 1.2 m/s, whereas the corresponding total pressure drop (Δp_b) decreased from 4.5 kPa to 4.2 kPa. With increasing the biomass fraction in the bed and static bed height, the difference between u_{mff} and u_{mpf} was apparently greater; however, like in the trials with pure alumina, the transition of the bed behavior from the static-bed regime to the fully fluidized-bed regime was accompanied by stepwise changes in superficial air velocity (u) and total pressure drop (Δp).

Fig. 6 depicts the Δp-u diagrams of the conical beds of alumina mixed with shredded oil palm shells of 7–10 mm particle sizes for the same ranges of the static bed height and biomass proportion in the binary mixture, as in Fig. 5. As compared between the two biomass particle sizes, the diagrams shown in Fig. 6 were quite similar to those in Fig. 5 and had minor effects of the biomass particle size. For the coarser biomass particles mixed with alumina sand, u_{mpf} and u_{mff} showed the trend to be slightly increased at the particular static bed height, likely in response to an increase in "effective" diameter of solid particles (averaged over the entire volume of a binary mixture). In the meantime, at fixed static bed height, the corresponding pressure drops – Δp_{max} and Δp_b – for the beds with coarser particles were a bit lower than those in Fig. 5 because of the lower bed weight.

Since the hydrodynamic characteristics at key points (A and B) for the two biomass particle size were nearly the same (at fixed static bed height and biomass proportion in the binary mixture), an appearance of the Δp-u dependencies for the two

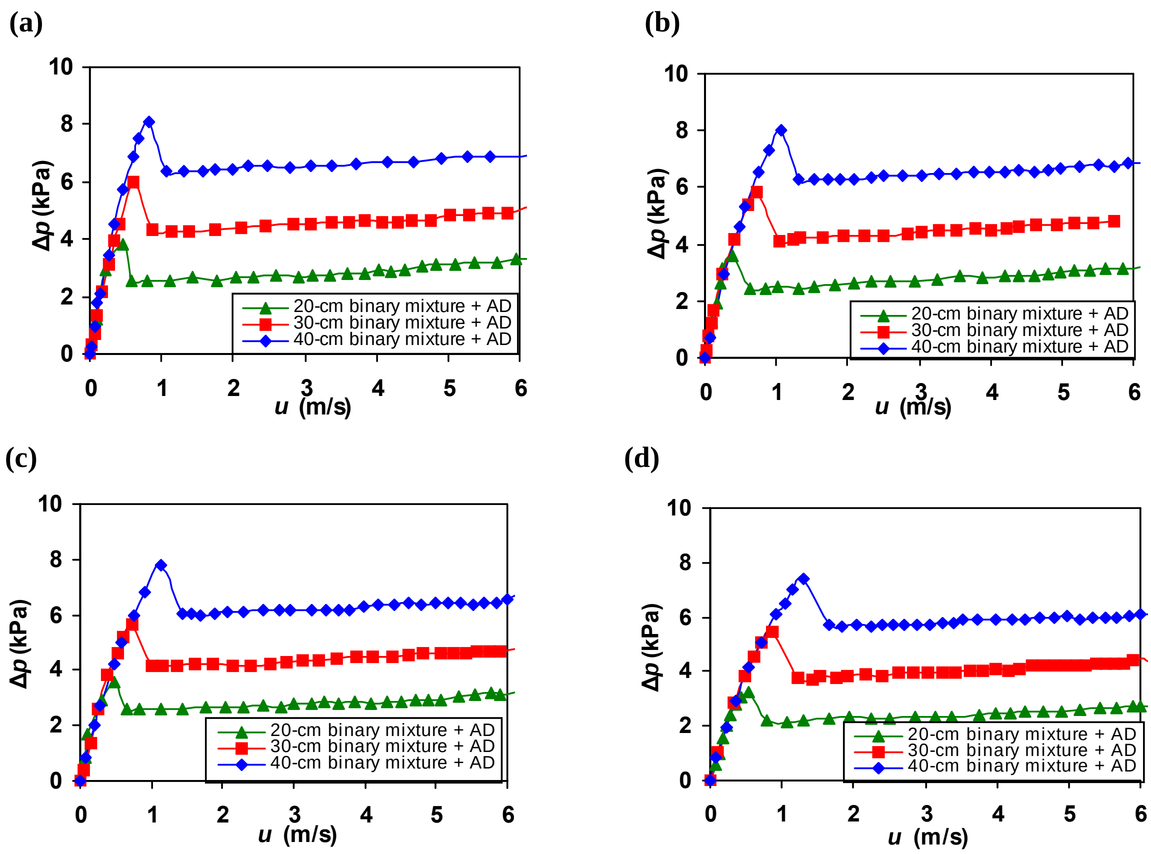

Fig. 6 Effects of static bed height on the Δp-u diagram of alumina mixed with shredded oil palm shells of 7−10 mm particle sizes for variable proportion of biomass in the binary mixture: (a) 2.5 wt.%, (b) 5.0 wt.%, (c) 7.5 wt.% and (d) 10 wt.%

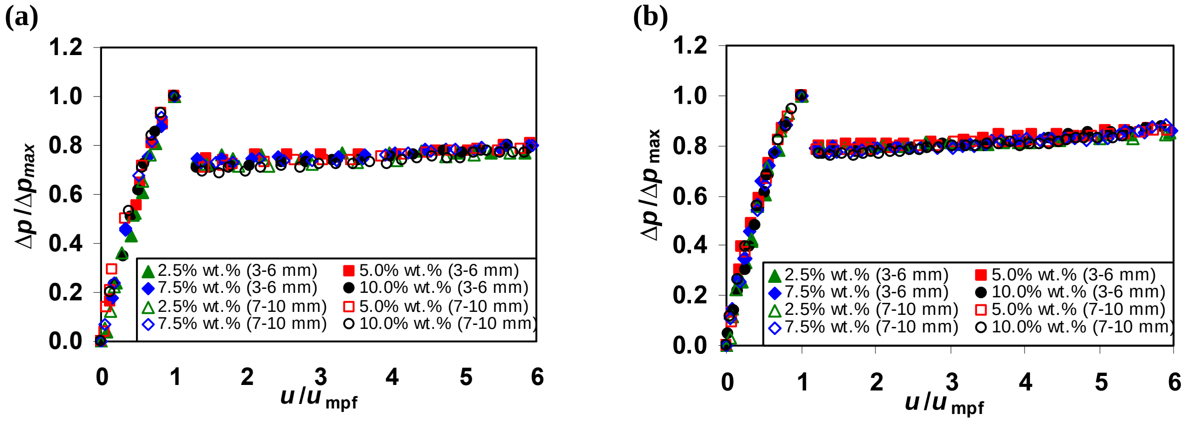

Fig. 7 Relative pressure drop across the bed versus relative superficial velocity at different wt.% and particle size of OPS mixed with alumina: (a) for BH = 30 cm, and (b) for BH = 40 cm

groups of particle sizes of the binary mixtures were quite similar.

With selected properties and characteristics of the bed material (alumina sand) and biomass (shredded oil palm shells), a stable fluidization (in bubbling or turbulent fluidized-bed regime) is expected to take place when burning oil palm shells in the proposed conical FBC in the range of fuel feed rate and air supply. Furthermore, a static bed height of 30 cm seems to be appropriate for this combustor as ensuring (i) stable fluidization of the bed (at reasonable u_{mff} and Δp_b), and (ii) sufficient amount of the bed material to sustain ignition and combustion of biomass fuels in the cone-shaped fluidized bed.

3.3 Relative hydrodynamic characteristics of the conical alumina-biomass beds

Fig. 7 shows the dependencies of the relative total pressure drop ($\Delta p/\Delta p_{max}$) on relative superficial air velocity (u/u_{mpf}) for variable percentage of biomass in the binary mixtures and biomass particle size for two static bed heights: 30 cm and 40 cm. It can be seen in Fig. 7 that, for each static bed height, the dependence $\Delta p/\Delta p_{max}$ = f(u/u_{mpf}), obtained via treatment of experimental data from different test runs, showed an apparent of the dimensionless curves. Within the fixed-bed region, $\Delta p/\Delta p_{max}$ versus u/u_{mpf} for the two static bed heights can be fitted by a single line with sufficient accuracy. Within the fully fluidized-bed region, the $\Delta p/\Delta p_{max}$ curves for distinct BHs were at different levels, exhibiting, however, nearly identical positive gradients, $d(\Delta p/\Delta p_{max})/d(u/u_{mpf})$, within this region, whose magnitudes are mainly affected by the contribution of the air distributor to the total pressure drop across the bed–distributor system. Thus, knowing the numerical values of u_{mpf} and Δp_{max} at critical point A for the particular operating variables (biomass percentage in the binary mixture, biomass particle size and static bed height, one can predict the total pressure drop (Δp) for any arbitrary superficial air velocity within the specified ranges of the operating variables (parameters).

3.4 Impact of hydrodynamic characteristics on operating regime of the conical FBC

The experimental procedure for firing shredded oil palm shells in the conical FBC included combustion tests at 45 kg/h fuel feed rate for the range of excess air of 20–100% [12]. This biomass fuel is characterized by the lower heating value of ~16 MJ/kg and requires ~4.9 Nm^3/kg stoichiometric air (under standard operating conditions: 1atm and 0°C). Using this theoretically required volume of air, it was estimated that to ensure the combustion of this biomass at the specified fuel feed rate and range of air supply, the superficial air velocity at the air distributor exit should be maintained in the range from 4.6 m/s to 7.7 m/s for firing OPS.

Based on the results from this cold-state hydrodynamic studies, for reasonable percentages of biomass in the binary mixture (2.5–5 wt.%) and selected static bed height (BH = 30 cm), the value of u_{mpf} for the two size groups of oil palm shells particles can be roughly estimated to be 0.6 m/s. So, in all tests for firing this biomass in the conical FBC, the superficial air velocity is to be maintained within (6–9)u_{mpf} for the specified range of excess air. Thus, the conical FBC was expected to ensure the turbulent fluidization regime in all combustion tests when burning 45 kg/h oil palm shells.

4. Conclusions

Hydrodynamic regimes and characteristics of a conical fluidized bed with variable (20–40 cm) static bed height have been studied under cold-state conditions in the special experimental rig reproducing a bottom part of the conical fluidized-bed combustor with a 40° cone angle. The behavior and characteristics of fluidization of the bed have been studied using alumina sand of 0.3–0.5 mm particle sizes mixed with shredded oil palm shells in different biomass fractions in the binary mixture (ranged from 0 to 10 wt.%). The experimental runs have been performed for two size groups of biomass particles: 3–6 mm and 7–10 mm.

The specific conclusions derived from this study are as follow:

- four sequent hydrodynamic regimes: (i) fixed-bed, (ii) partially fluidized-bed, (iii) fully fluidized-bed and (iv) turbulent fluidized-bed regimes occur in the gas–solid bed when increasing superficial air velocity from 0 to 6 m/s;
- the proposed air distributor with nineteen bubble caps closely arranged on the distributor plate ensures a rather low pressure drop across the distributor and uniform distribution of airflow over the plate and consequently across the conical fluidized bed.
- with increasing static bed height, the major hydrodynamic characteristics of alumina (or alumina–biomass) beds – the minimum velocity of full fluidization (u_{mff}) and the corresponding total pressure drop across the air distributor and the bed (Δp_b) – show the trend to be increased;
- with greater proportion of biomass in the binary mixture, u_{mff} shows the trend to be slightly increased, whereas Δp_b exhibits a small reduction;
- particle size of shredded oil palm shells in the binary mixture has quite weak effects on the major hydrodynamic characteristics;
- the dimensionless dependency of $\Delta p/\Delta p_{max}$ on u/u_{mpf} for all binary mixtures showed a similarity for the ranges of biomass fraction in the binary mixture, biomass particle size and static bed height;
- with selected properties and characteristics of the bed material and oil palm shells and taking into account static bed height, a stable fluidization (likely, in turbulent fluidized-bed regime) is expected to take place when burning shredded oil palm shells in the proposed conical fluidized bed combustor operated with the excess air of 20–100%.

5. Acknowledgements

The authors wish to acknowledge the financial support from the Bangchak Petroleum Public Company Limited.

6. References

[1] Kaewklum, R.. and Kuprianov, V.I. (2008). Theoretical and experimental study on hydrodynamic characteristics of fluidization in air–sand conical beds. *Chemical Engineering Science*, vol. 63, pp. 1471–1479.

[2] Geldart, D. (1973). Types of gas fluidization, Powder Technology, vol. 7, pp. 285–292.

[3] Kunii, D. and Levenspiel, O. (1991). Fluidization Engineering, Butterworth-Heinemann, Boston.

[4] Peng, Y. and Fan, L.T. (1997). Hydrodynamic characteristics of fluidization in liquid-solid tapered beds, *Chemical Engineering Science*, vol. 52, pp. 2277–2290.

[5] Jing, S. Hu, Q. Wang, J. and Jin, Y. (2000). Fluidization of coarse particles in gas–solid conical beds, *Chemical Engineering and Processing*, vol. 39, pp.379–387.

[6] Permchart, W. and Kouprianov, V.I. (2004). Emission performance and combustion efficiency of a conical fluidized-bed combustor firing various biomass fuels, *Bioresource Technology*, vol. 92, pp. 83–91.

[7] Arromdee P. and Kuprianov, V.I. (2012). Combustion of peanut shells in a cone-shaped bubbling fluidized-bed combustor using alumina as the bed material. *Applied Energy*, vol. 97, pp. 470–482.

[8] Rao, T.R. and Ram Bheemarasetti, J.V. (2001). Minimum fluidization velocities of mixtures of biomass and sands, *Energy*, vol. 26, pp. 633–644.

[9] Zhang, Y., Jin, B. and Zhong, W. (2009). Experimental investigation on mixing and segregation behavior of biomass particle in fluidized bed. *Chemical Engineering and Processing*, 48: 745–754.

[10] Sun, Z., Jin, B., Zhang, M., Liu, R. and Zhang, Y. (2008). Experimental studies on cotton stalk combustion in a fluidized bed. *Energy*, 33: 1224–1232.

[11] Shimizu, T., Han, J., Choi, S., Kim, L. and Kim, H. (2006). Fluidized-bed combustion characteristics of cedar pellets by using an alternative bed material, *Energy & Fuels*, vol. 20, pp. 2737-2742.

[12] Ninduangdee, P. and Kuprianov, V. I. (2012). Measures for reliable and effective operation of a conical fluidized-bed combustor fired with oil palm shells: A combustion study. In: *Proceedings of The Third TSME Conference on Mechanical Engineering* (in this volume).